Integrated Visualization of Diffusion Tensor Fiber Tracts and Anatomical Data

Dorit Merhof[*†], Frank Enders[*†], Fernando Vega[*†], Peter Hastreiter[*†], Christopher Nimsky[‡], Marc Stamminger[*]

Abstract

Diffusion tensor imaging allows to investigate white matter structures in vivo which is of particular interest for neurosurgery. However, due to the restricted resolution of the data and due to noise artifacts the analysis of this kind of data is a challenging task. A promising approach for the reconstruction of neural pathways are streamline based approaches commonly referred to as fiber tracking. In this paper we present our tracking algorithm as well as an integrated visualization approach for fibers and anatomical data that takes into account the requirements for clinical application.

1 Introduction

Diffusion tensor imaging (DTI) provides the diffusion characteristics of water molecules within tissue. Due to the long cylindric shape of axons, water diffusion is anisotropic within fibrous material. Contrarily, in areas of grey matter the diffusion probability is equally distributed since rather round grey matter cells dominate. DTI thus enables to reconstruct white matter anatomy to study neural structures within the human brain. The directional variation of diffusion is measured for at least six non-collinear gradient directions. These diffusion images serve as a basis for the computation of diffusion tensors. The resulting second order tensors characterize the diffusion probabilities within tissue. To exploit the contained information most approaches utilize the eigensystem of each tensor:

2D slice images of diffusion measures derived from the eigensystem components such as fractional anisotropy (FA) [BMP+01] or c_l, c_p, c_s (linear, planar and spherical diffusion) [WMM+02] already show diffusion characteristics of the material. However, direct volume visualization of these diffusion measures [KWH00] does not lead to valuable representations for surgery. This also applies to the iso-surfaces of the data. A further 2D representation of diffusion are hue-balls [KW99] which color encode the deflection of a predefined vector after multiplication with the tensor using a grey-scale or color-scale sphere.

Glyph-based approaches directly visualize eigenvectors and eigenvalues of the tensor using ellipsoids which may be drawn in real-time using hardware-acceleration [EIBH+05]. An even better shape for representing diffusion tensors are superquadrics [Kin04]. A severe disadvantage of this approach is that superquadrics are computed in software which is currently not possible in real-time.

[*]Computer Graphics Group, University of Erlangen, Am Weichselgarten 9, 91058 Erlangen, Germany
[†]Neurocenter, Dept. of Neurosurgery, University of Erlangen, Schwabachanlage 6, 91054 Erlangen, Germany
[‡]Dept. of Neurosurgery, University of Erlangen, Schwabachanlage 6, 91054 Erlangen, Germany

Fiber tracking which is maybe the most appealing and understandable technique for representing white matter has been investigated by several groups [MCCvZ99, BPP$^+$00, SKvZ$^+$01, MvZ02, ZB02, FGLG03, VBvP04]. All these approaches are based on streamline techniques known from flow visualization. Thereby, the respective vector field is derived by taking the major eigenvector of each tensor. Fiber tracking algorithms often utilize thresholds, angle criterions, regularization techniques and local filters to improve tracking results.
However, all these visualization approaches for white matter structures should be evaluated considering their capacities for surgical planning. 2D representations of FA and c_l, c_p, c_s as well as hue balls are already able to show spatial relations between lesions and white matter. Volume visualization or iso-surfaces of these diffusion measures do not further improve the quality of representation for clinical purposes. Glyph visualization on the other hand is of interest for investigating tumor borders and infiltration of white matter tracts. A really useful tool for surgical planning are fiber tracts computed by streamline based approaches since they are a very comprehensive representation of the data. A combined visualization of fiber tracts and anatomy which is outlined in more detail in this paper is a very promising tool for assisting in surgical planning. The concurrent display of anatomy and fibers enables the surgeon to assess the location of fibers in relation to anatomical landmarks. This is of major importance in patients with space occupying lesions which may cause a displacement of fibers and other anatomical structures.

2 Image Data

In addition to directional diffusion images required for computing fibers, anatomical data is needed for fusion. A T1 weighted MR sequence such as MPRAGE (Magnetization Prepared Rapid Acquisition Gradient Echo) provides the required anatomical detail. All images were acquired using a Siemens MR Magnetom Sonata Maestro Class 1.5 Tesla scanner equipped with a gradient system with a field strength of up to 40 mT/m (effective 69 mT/m) and a slew rate of up to 200 T/m/s (effective 346 T/m/s). Regarding image acquisition for DTI, the scanner is able to generate images for six or alternatively twelve diffusion directions.

DT image data: The diffusion images differed in the direction of the gradient that was applied. For each slice a total amount of seven images was created: One reference image was measured without any gradient direction which is equivalent to common T2 weighted MR data. The remaining six or alternatively twelve images were acquired using different gradient directions that correspond to the diffusion directions measured at that time. With respect to anatomical information, the reference image represents anatomical structures best though in poor detail. The other images show diffusion properties.

DT imaging parameters: TR = 9200, TE = 86 ms, b_{high} = 1000 s/mm^2, b_{low} = 0 s/mm^2, field of view 240 mm, voxel size 1.875$\times$1.875$\times$1.9 mm^3, 1502 Hz/Px bandwidth, acquisition matrix 128$\times$128, 60 slices. The diffusion-encoding gradients for the six diffusion weighted images were directed along the following axes: ($\pm$1,1,0), ($\pm$1,0,1) and (1,$\pm$1,0).

MPRAGE image data: The advantages of this modality are a high signal to noise ratio, thin coherent slices and the possibility of multi-planar reconstruction.

MPRAGE imaging parameters: TR = 2020 ms, TE = 4.38 ms, field of view 250 mm, voxel size $0.488281 \times 0.488281 \times 1.0\,\mathrm{mm}^3$, acquisition matrix 512×512, 128 slices.

3 Methods

The main challenge of medical visualization is to show the required information for diagnosis and therapy planning in an unambiguous and intuitive manner. In the case of DTI, the visualization of fiber streamlines in combination with high quality anatomical data is a promising step towards this objective. This kind of visualization is of special interest for surgical planning in neurosurgery. To avoid postoperative neurological deficits a surgeon must be able to estimate the spatial relation between tumor and vital white matter structures. An integrated visualization of fiber tracts and anatomical data is a valuable contribution to safer surgery.
This chapter starts with a short introduction to data processing (Section 3.1) and fiber tracking (Section 3.2). The main focus is on different visualization aspects which are treated in Section 3.3.

3.1 Data processing

The different diffusion datasets and the slice numbering within each dataset have to be identified using the tags available within the DICOM (Digital Imaging and Communications in Medicine) headers.
Taking the six datasets with different gradient directions and the dataset that was measured without any gradient a second order diffusion tensor was computed for each voxel by solving the Stejskal-Tanner equations system [ST65]

$$S_i = S_o \, \mathrm{e}^{-b \, \hat{\mathbf{g}}_i^T \mathbf{D} \hat{\mathbf{g}}_i} \, .$$

Thereby, $\mathbf{D}$ is the diffusion tensor for a voxel that has to be computed, S_i is the measured diffusion value of this voxel for dataset i, S_o represents the value of this voxel within the dataset without gradient, $\hat{\mathbf{g}}$ stands for the gradient direction of dataset i and b is LeBihan's b-factor which depends on several image acquisition parameters. Since the second order diffusion tensors are symmetric, the six unknowns within each tensor are uniquely defined in the case of six gradient directions. An efficient way for solving the equations system is outlined in [WMM$^+$02].
A set of filters was implemented to deal with imaging noise. The filters are applied component-wise for all tensors. More precisely, the filter is first applied to all first entries of the tensors, then to all second entries and so on. Currently, our set of filters comprises a Gaussian-filter as well as a non-linear edge enhancing filter and a best-neighbor filter [ZPV02]. For all filters the kernel size may be defined by the user. In case of the Gaussian-filter, the filter kernel components are derived by determining the corresponding binomial coefficients. The non-linear edge enhancing filter computes the difference

between the tensor entry of a voxel and its neighboring voxels. Depending on the similarity of these values each neighbor is weighted. In this way, similar values have a higher contribution to the filtered value. The third filter, a best-neighbor filter, works in a similar way. Surrounding neighbors are sorted according to the difference of values. Only the best-matching third of the sorted neighbors is equally weighted and contributes to the filtered value of the center voxel. A comparison of the filter results is shown in Figure 1 where axial slice images of FA are presented.

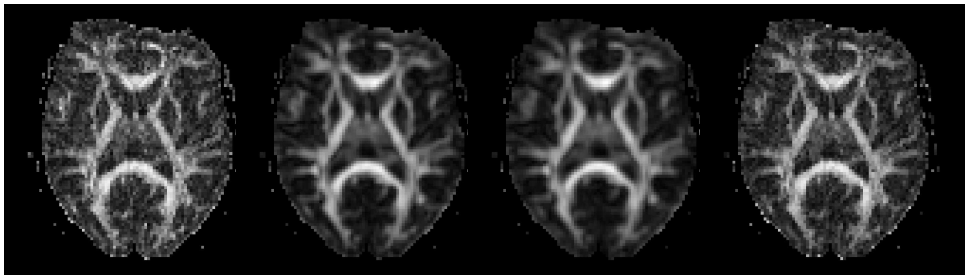

Figure 1: Comparison of different filters, axial slices of FA dataset after filtering of diffusion tensors are presented. Filters from left to right (filter kernel size 3): Original, Gaussian filter, non-linear edge enhancing filter, best-neighbor filter

3.2 Fiber tracking

A very popular approach for visualizing diffusion tensors is to perform fiber tracking. The streamlines extracted by tracking algorithms are assumed to represent the most likely pathways through the tensor field. Note that the term 'fibers' is used for streamlines which do not represent real anatomical fibers but provide an abstract model of neural structures. Starting from seed voxels, the tracking is performed in forward and backward direction with sub-voxel precision. For the selection of seed voxels and for aborting the streamline propagation, FA is used as a threshold. FA represents the degree of anisotropic diffusion and therefore is a proper measure for the probability of white matter. Following this assumption, voxels with high FA are used as seed voxels. If FA falls below a certain threshold, the tracking stops.
Accordingly, a single tracking step of the streamline propagation looks as follows: The tensor at the current end point of the fiber is computed using trilinear interpolation which is separately performed for each tensor entry. The eigensystem of the tensor is then determined. The eigenvector belonging to the highest eigenvalue, in the following referred to as principal eigenvector, correlates with the direction of highest diffusion. In case of Euler integration, the next streamline propagation step would be in direction of this principal eigenvector. For reasons of numerical accuracy, we apply a higher order integration scheme (Runge-Kutta of order four) which needs repeated tensor interpolation and principal eigenvector computations until the direction of streamline propagation is determined.

The step size is set to a fixed value which is a quarter of the voxel size. Since the field of the principal eigenvectors does not correspond to a flow field we found it more convenient to choose a sufficiently low fixed step size instead of adaptive adjustments. Contrarily to nerves, flows consisting of particles posses physical properties such as inertia which ensure that sudden changes of direction do not occur. For fiber tracking a fixed step size is safer to prevent missing turnoffs. Apart from the FA threshold for aborting fiber tracking, streamline propagation is aborted in the subsequently described cases. If a streamline has reached a maximum length or if the angle between the last two steps is above a certain threshold, tracking stops. A further criterion for accepting a fiber is its length. Streamlines are rejected if they are below a minimum length. Beside these thresholds the user may choose between a tracking encompassing the whole brain or a tracking extracting fibers that run through user-defined regions of interest (ROIs). The latter approach enables the reconstruction of separate tract systems which is of special interest for medical applications.

3.3 Visualization

The visualization of neural pathways for medical applications has to fulfill several criteria. For planning of brain tumor surgery one has to investigate the spatial relation between tumor and fibers. This was achieved using a concurrent display of fibers and anatomical data which was either represented in a single slice or with direct volume rendering. The rendering of fibers is discussed in Section 3.3.1, the direct volume rendering is described in Section 3.3.2. Important aspects for the fusion of fibers and anatomical data are outlined in Section 3.3.3.

3.3.1 Fibers

The OpenGL API was used for rendering the fibers. Thereby, each tract was stored as a vertex array and drawn as a set of lines. The standard strategy for color encoding of fibers [CLV+94, JWH97, PP99] is to utilize the normalized principal eigenvector components of the local trilinear interpolated tensor as RGB values. Here, we used a simplified approach employing the components of the normalized vector which connects two subse-

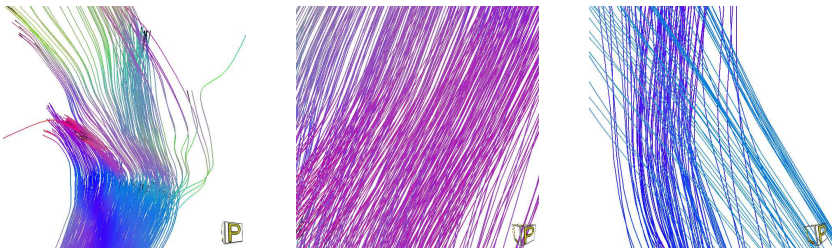

Figure 2: Closeups of a pyramidal tract. Standard color encoding is achieved using vector between adjacent tracking points.

quent fiber points to avoid trilinear tensor interpolation and eigen analysis. Since the step size for tracking is sufficiently small, the visual impression remains the same.
A further strategy to improve streamline visualization could be to incorporate illumination of the fibers. However, practical experience has shown that it is better to omit any illumination. It modifies color encoding and thus falsifies the color information which in combination with the 3D representation of fibers already provides a good spatial impression. Any contribution to a better estimation of the shape of fibers using illumination is hardly observable.

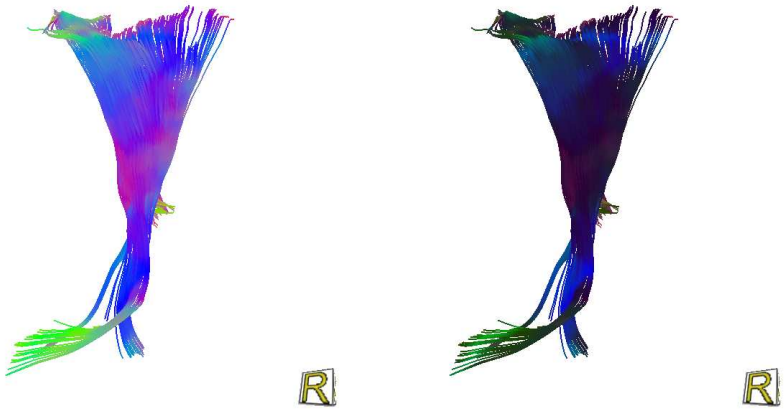

Figure 3: Illumination of fibers modifies color information and is therefore not recommended in case of single track visualization. *Left:* Fiber without illumination. *Right:* Illuminated fiber.

3.3.2 Volume Rendering

The concurrent display of anatomical MR data and fibers is achieved with direct volume rendering. This is supported by the capabilities of current PC graphics hardware. It is capable to handle volume data as 3D textures and enables interactive visualization. Apart from investigating slice images of the data, 3D volume rendering of clinical data is suited to get an intuitive impression of the spatial relations of anatomical landmarks. Therefore, it is a valuable tool for investigation and planning in brain tumor surgery.
However, visualizing MR data using direct volume rendering is difficult due to the low dynamic range of intensity values. Additionally, different anatomical structures such as skin and brain tissue are represented by the same intensity value which prevents the separation of different structures using intensity based transfer functions. Therefore, an alternative strategy for visualizing and investigating the spatial relation of fibers and anatomy or brain tumors are tagged volumes. For this purpose, relevant structures such as the ventricles or a brain tumor were segmented in a preprocessing step. Thereby, a second dataset containing tag ids for each part was generated which allowed assigning specific transfer functions to each sub-volume. Figure 4 shows a brain tumor that is rendered as tagged volume.

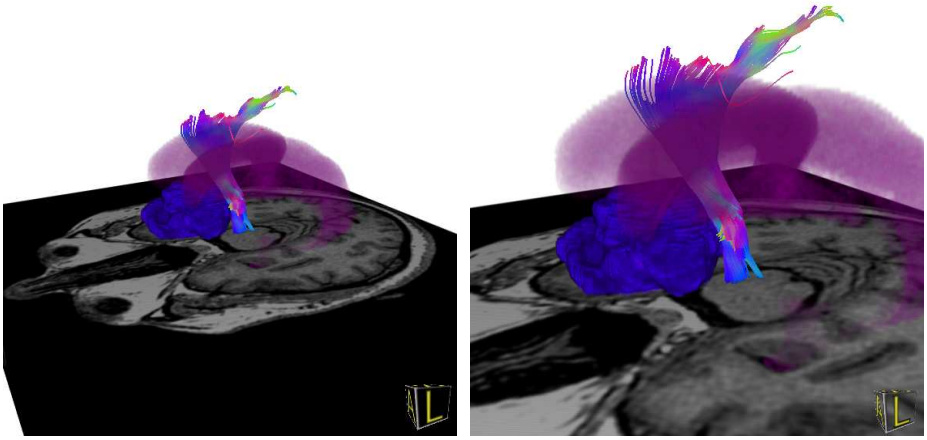

Figure 4: Tagged volume visualization applying separate transfer functions for a tumor *(blue)*, ventricles *(red)* and surrounding tissue combined with closely related fibers represented with lines.

In addition to tagged volumes clipping is essential since it allows suppressing entire areas from rendering and thereby gives direct visual access to hidden structures. Therefore, hardware accelerated clipping of arbitrary geometry as introduced by Weiskopf [WEE02] was incorporated in order to allow masking of uninteresting areas. Combining tagged volumes with clipped volume rendering allows investigating segmented structures and surrounding anatomy which may be combined with rendered fibers. This led to clear visualizations as shown in Figure 5.

3.3.3 Fusion

The current restriction to opaque fibers allowed a simple step-by-step rendering. After rendering the fibers, back-to-front rendering of the volume with activated depth buffer was sufficient. Parts of the volume which were concealed by the fibers were suppressed by the depth-test. Further extensions towards semi-transparent fiber representations will be computationally more expensive since depth sorting has to be applied.
High accuracy with respect to showing the spatial relation of fibers and anatomy is a common goal for all visualization strategies. While merging fibers with the corresponding reference dataset is trivial, for other image data such as MPRAGE this is a difficult task. In this case, registration has to be applied prior to visualization to adjust the datasets. Rigid registration is thereby sufficient for many registration tasks dealing with undistorted image data. In the case of DTI, non-linear registration has to be performed to account for image distortions of the DTI sequence. Non-linear registration thus ensures that fibers computed from the distorted DTI images are positioned properly within the undistorted dataset showing anatomy [MHS+04]. Alternatively, if non-linear registration is omitted, the observer has to take into account that fibers are positioned with a certain error.

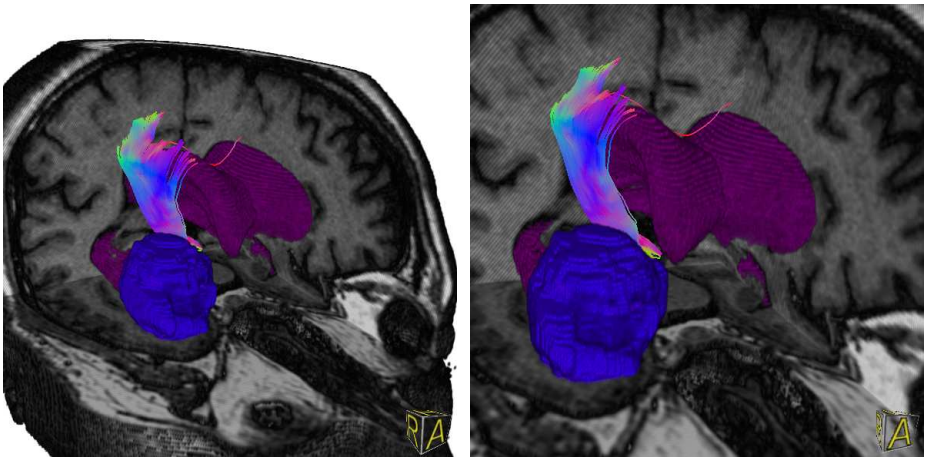

Figure 5: Improved anatomical orientation using visualization of tagged data based on volume clipping combined with fibers represented with lines.

4 Results

The presented approach for an integrated visualization of diffusion tensor fiber tracts and anatomical data was adapted to application in surgery. In addition to 2D slice image sequences, direct volume rendering provides a better understandable representation of 3D anatomy. Volume clipping is thereby an essential tool for investigating inner structures which are hardly discoverable with intensity based transfer functions. Since different anatomical structures occupy identical grey values and the differences between grey values are low, volume clipping has prior importance compared to transfer functions. Interactive adjustment of the clip volume thereby provides fast and precise access to inner structures. A combined rendering of clipped anatomical data and fiber lines thus allows investigating the course of fibers and nearby anatomy simultaneously. If a 3D representation of certain structures is recommended, the desired areas are segmented by an clinical expert and rendered as tagged volumes. Regarding the visualization of brain tumors, this approach is superior compared to a transfer function based visualization as brain tumors often have no clear border due to infiltration with other tissue. A tagged volume approach clearly shows the volume of the tumor. Thus, it is much more appropriate for investigating the spatial relation of tumor, fibers and anatomy which is essential for surgery. The integrated visualization approach hence provides a comprehensive representation of the complex 3D data and fiber anatomy.

Regarding performance aspects the aim was to enable interactive manipulation and comfortable handling of the tools. The computation of fibers which lasts up to one minute for a whole brain is the most time consuming part. The volume rendering and application of transfer functions, tagged volumes and clipping run interactively due to extensive use of

graphics hardware. The frame rates for a number of setups using different graphics cards are presented in Table 1. We measured the frame rates for displaying two different tract systems and a tracking of the whole brain in combination with a DTI reference dataset and MPRAGE anatomical datasets. The tract systems (pyramidal tract and optical tract) contained about 240 and 330 fibers, the tracking of the whole brain resulted in 3980 fibers. The average number of tracked points for each fiber was about 160. The dimensions of the datasets were $128\times128\times60$ voxel for the DTI reference dataset and $256\times256\times128$ and $512\times512\times128$ voxel for the MPRAGE anatomical datasets. For measuring frame rates we used PCs equipped with an Intel Pentium 4 (3 GHz) and GeForce FX 5700, GeForce FX 5950, GeForce 6800 Ultra and GeForce Quadro FX 1000 graphics cards.
These results show that investigating anatomy and fibers interactively is possible. This is of major importance for clinical application due to limited time in clinical workflows which highly influences the acceptance of medical tools.

GeForce FX 5700	Pyramidal tract	Optical tract	Whole brain
DTI 128	12.4	12.1	4.7
MPRAGE 256	7.8	7.7	3.7
MPRAGE 512	3.3	3.3	2.4

GeForce FX 5950	Pyramidal tract	Optical tract	Whole brain
DTI 128	46.1	45.0	6.6
MPRAGE 256	24.0	23.6	5.9
MPRAGE 512	9.8	9.8	4.4

GeForce 6800 Ultra	Pyramidal tract	Optical tract	Whole brain
DTI 128	125.0	122.0	5.8
MPRAGE 256	47.8	47.5	5.5
MPRAGE 512	20.5	20.2	4.8

GeForce Quadro FX 1000	Pyramidal tract	Optical tract	Whole brain
DTI 128	36.8	36.8	7.5
MPRAGE 256	22.3	22.0	6.4
MPRAGE 512	8.2	8.1	4.3

Table 1: Frame rates in fps for different setups and different graphics cards.

5 Conclusion

In neurosurgery, extensive pre-operative planning is performed to minimize the risk of surgery. In this context, it is of major importance for the physician to collect information about the spatial relation between a tumor or aneurysm and neural pathways, major veins or speech areas. An appropriate visualization of neural fibers in addition to volume rendering

of anatomical data enhanced with clipping or tagged volumes provides the needed flexibility for obtaining a meaningful visualization. Overall, the presented visualization techniques are capable to support diagnosis and planning in surgery.

6 Acknowledgments

This work was supported by the Deutsche Forschungsgemeinschaft in the context of SFB 603, Project C9 and the Graduate Research Center "3D Image Analysis and Synthesis".

References

[BMP+01] D. Le Bihan, J.-F. Mangin, C. Poupon, C. Clark, S. Pappata, N. Molko and H. Chabriat. *Diffusion Tensor Imaging: Concepts and Applications*. Magnetic Resonance Imaging, 2001.

[BPP+00] P. Basser, S. Pajevic, C. Pierpaoli, Jeffrey Duda and Akram Aldroubi. *In Vivo Fiber Tractography Using DT-MRI Data*. Magnetic Resonance in Medicine, 44:625–632, 2000.

[CLV+94] J. Coremans, R. Luypaert, F. Verhelle, T. Stadnik and M. Osteaux. *A Method for Myelin Fiber Orientation Mapping Using Diffusion-Weighted MR Images.* Magnetic Resonance Imaging, pp. 443–454, 1994.

[EIBH+05] F. Enders, S. Iserhardt-Bauer, P. Hastreiter, C. Nimsky and T. Ertl. *Hardware-Accelerated Glyph Based Visualization of Major White Matter Tracts for Analysis of Brain Tumors*. In: Proc. SPIE Medical Imaging, 2005. Accepted for publication.

[FGLG03] P. Fillard, J. Gilmore, W. Lin and G. Gerig. *Quantitative Analysis of White Matter Fiber Properties along Geodesic Paths*. In: Proc. MICCAI, 2003.

[JWH97] D. Jones, S. Williams and M. Horsfield. *Full Representation of White-Matter Fibre Direction in One Map via Diffusion Tensor Analysis*. In: Proc. 5th Int. Soc. of Mag. Res. in Med., pp. 1743, 1997.

[Kin04] G. Kindlmann. *Superquadric tensor glyphs*. In: Proc. IEEE Visualization, 2004.

[KW99] G. Kindlmann and D. Weinstein. *Hue-Balls and Lit-Tensors for Direct Volume Rendering of Diffusion Tensor Fields*. In: Proc. IEEE Visualization, pp. 183–189, 1999.

[KWH00] G. Kindlmann, D. Weinstein and D. Hart. *Strategies for Direct Volume Rendering of Diffusion Tensor Fields*. IEEE Transactions on Visualization and Computer Graphics, 6(2):124–138, 2000.

[MCCvZ99] S. Mori, B. Crain, V. Chacko and P. van Zijl. *Three-dimensional tracking of axonal projections in the brain by magnetic resonance imaging*. Ann Neurol, 45(2):265–269, February 1999.

[MHS+04] D. Merhof, P. Hastreiter, G. Soza, M. Stamminger and C. Nimsky. *Nonlinear Integration of DTI-based Fiber Tracts into Standard 3D MR Data*. In: Proc. Vision, Modeling, and Visualization (VMV), pp. 371–377. Akademische Verlagsgesellschaft Aka, Berlin, 2004.

[MvZ02] S. Mori and P. van Zijl. *Fiber tracking: principles and strategies – a technical review*. NMR Biomed, 15:468–480, 2002.

[PP99] S. Pajevic and C. Pierpaoli. *Color schemes to represent the orientation of anisotropic tissues from diffusion tensor data: Application to white matter fiber tract mapping in the human brain*. Magnetic Resonance in Medicine, 42(3):526–540, 1999.

[SKvZ+01] B. Stieltjes, W. Kaufmann, P. van Zijl, K. Fredericksen, G. Pearlson, M. Solaiyappan and S. Mori. *Diffusion tensor imaging and axonal tracking in the human brainstem*. NeuroImage, 14:723–735, 2001.

[ST65] E. Stejskal and J. Tanner. *Spin diffusion measurements: spin echoes in the presence of a time-dependent field gradient*. J. Chem. Phys., 42:288–292, 1965.

[VBvP04] A. Vilanova, G. Berenschot and C. van Pul. *DTI Visualization with Streamsurfaces and Evenly-Spaced Volume Seeding*. In: Proc. Joint EG/IEEE TCVG VisSym, pp. 173–182, 2004.

[WEE02] D. Weiskopf, K. Engel and T. Ertl. *Volume Clipping via Per-Fragment Operations in Texture-Based Volume Visualization*. In: Proc. IEEE Visualization, 2002.

[WMM+02] C. Westin, S. Maier, H. Mamata, A. Nabavi, F. Jolesz and R. Kikinis. *Processing and visualization for diffusion tensor MRI*. Med Image Anal, 6(2):93–108, 2002.

[ZB02] L. Zhukov and A. Barr. *Oriented Tensor Reconstruction: Tracing Neural Pathways from Diffusion Tensor MRI*. In: Proc. IEEE Visualization, 2002.

[ZPV02] V. Zlokolica, W. Philips and D. Van De Ville. *A new non-linear filter for video processing*. In: Proc. 3rd IEEE Benelux Signal Processing Symposium (SPS), pp. S02–1 – S02–4, 2002.

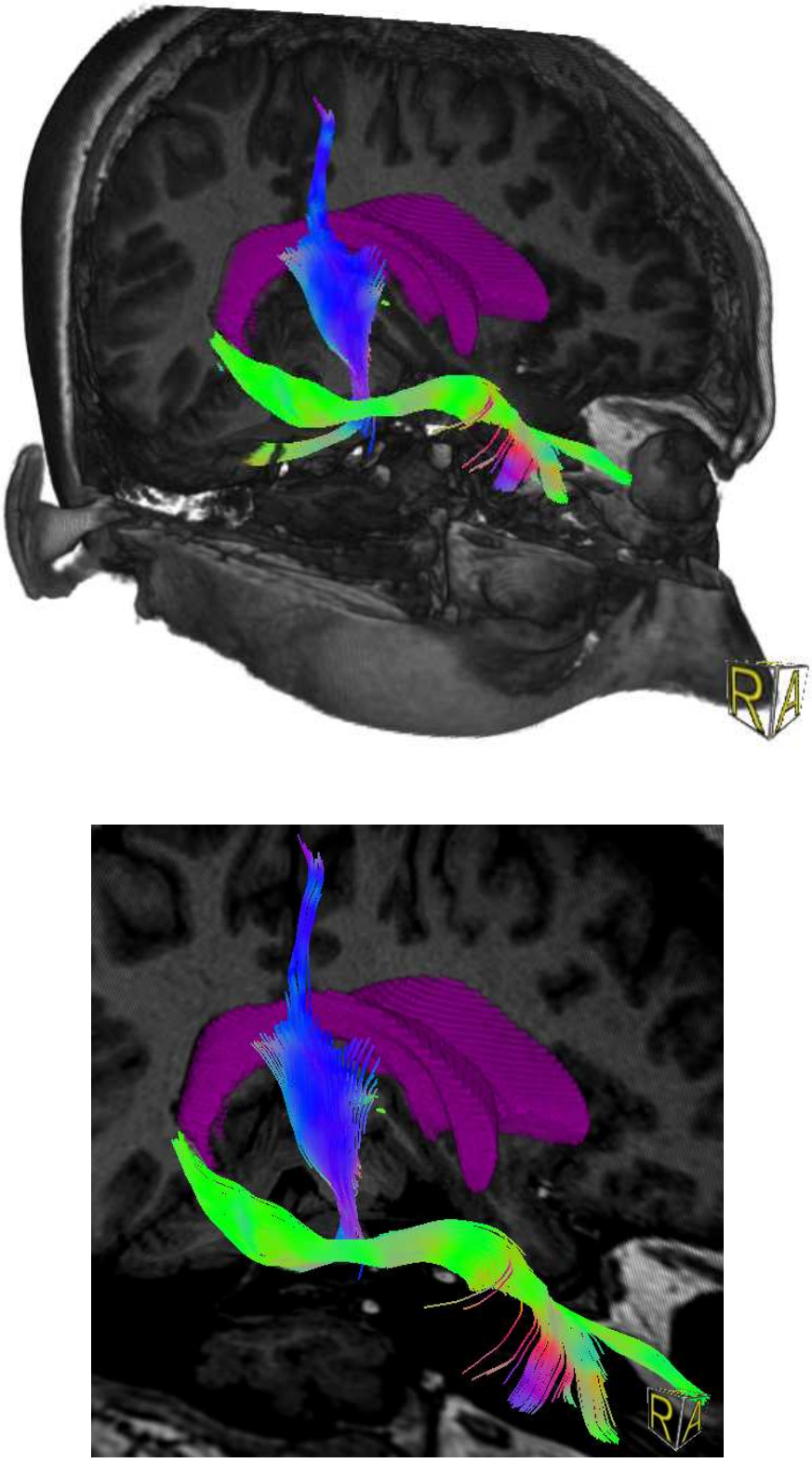

Figure 6: Combined visualization of fibers and anatomy in a healthy volunteer. Pyramidal tract *(blue)* and optical tract *(green)* represented with lines. Ventricles *(magenta)* are displayed utilizing tagged data.